

## Quantitative structure activity relationship studies on the flavonoid mediated inhibition of multidrug resistance proteins 1 and 2

Jelmer J. van Zanden<sup>a,\*</sup>, Heleen M. Wortelboer<sup>b</sup>, Sabina Bijlsma<sup>b</sup>, Ans Punt<sup>a</sup>, Mustafa Usta<sup>b</sup>, Peter J. van Bladeren<sup>c,d</sup>, Ivonne M.C.M. Rietjens<sup>a,c</sup>, Nicole H.P. Cnubben<sup>b</sup>

<sup>a</sup>Division of Toxicology, Wageningen University, P.O. Box 8000, 6700 EA Wageningen, The Netherlands

<sup>b</sup>TNO Nutrition and Food Research, P.O. Box 360, 3700 AJ Zeist, The Netherlands

<sup>c</sup>TNO Centre for Food Toxicology, Wageningen University, P.O. Box 8000, 6700 EA Wageningen, The Netherlands

<sup>d</sup>Nestlé Research Centre, P.O. Box 44, CH-1000 Lausanne 26, Switzerland

Received 25 June 2004; accepted 8 November 2004

### Abstract

In the present study, the effects of a large series of flavonoids on multidrug resistance proteins (MRPs) were studied in MRP1 and MRP2 transfected MDCKII cells. The results were used to define the structural requirements of flavonoids necessary for potent inhibition of MRP1- and MRP2-mediated calcein transport in a cellular model. Several of the methoxylated flavonoids are among the best MRP1 inhibitors ( $IC_{50}$  values, ranging between 2.7 and 14.3  $\mu$ M) followed by robinetin, myricetin and quercetin ( $IC_{50}$  values ranging between 13.6 and 21.8  $\mu$ M). Regarding inhibition of MRP2 activity especially robinetin and myricetin appeared to be good inhibitors ( $IC_{50}$  values of 15.0 and 22.2  $\mu$ M, respectively). Kinetic characterization revealed that the two transporters differ marginally in the apparent  $K_m$  for the substrate calcein. For one flavonoid, robinetin, the kinetics of inhibition were studied in more detail and revealed competitive inhibition with respect to calcein, with apparent inhibition constants of 5.0  $\mu$ M for MRP1 and 8.5  $\mu$ M for MRP2. For inhibition of MRP1, a quantitative structure activity relationship (QSAR) was obtained that indicates three structural characteristics to be of major importance for MRP1 inhibition by flavonoids: the total number of methoxylated moieties, the total number of hydroxyl groups and the dihedral angle between the B- and C-ring. Regarding MRP2 mediated calcein efflux inhibition, only the presence of a flavonol B-ring pyrogallol group seems to be an important structural characteristic. Overall, this study provides insight in the structural characteristics involved in MRP inhibition and explores the differences between inhibitors of these two transporters, MRP1 and MRP2. Ultimately, MRP2 displays higher selectivity for flavonoid type inhibition than MRP1.

© 2004 Elsevier Inc. All rights reserved.

**Keywords:** MRP1; MRP2; Flavonoids; QSAR; Calcein

### 1. Introduction

Membrane proteins belonging to the ATP-binding cassette family of transport proteins play a central role in the defense of organisms against toxic compounds [1,2]. The multidrug resistance proteins (MRPs) belong to this family, consisting of nine members, which differ widely in substrate specificity, tissue distribution and intracellular loca-

tion [3]. The first cloned member of this family, MRP1 (ABCC1) has a broad substrate specificity including glutathione S-conjugates, glucuronide conjugates, sulphate conjugates, anticancer drugs, heavy metals, organic anions and lipid analogues [4–6]. MRP1 is considered a prototype GS-X pump because of the important role of glutathione (GSH) for its transport action. Besides the transport of glutathione S-conjugates, the efflux of many substrates, like the oxyanions arsenite and antimonite and some drugs like vincristine and daunorubicin, are stimulated by or co-transported with glutathione [7–10]. MRP2 (ABCC2), the major canalicular multispecific organic anion transporter, is closely related to MRP1 [3,11]. Nevertheless, the tissue localization of these two transporters differs. Whereas

*Abbreviations:* MRP, multidrug resistance protein; GSH, glutathione; GS-X, glutathione conjugate;  $IC_{50}$ , 50% inhibition concentration; P-gp, P-glycoprotein; QSAR, quantitative structure activity relationship

\* Corresponding author. Tel.: +31 317 482294; fax: +31 317 484931.

E-mail address: [jelmer.vanzanden@wur.nl](mailto:jelmer.vanzanden@wur.nl) (J.J. van Zanden).

MRP1 is localized in the basolateral membranes of polarized cells and is present in all tissues, MRP2 is found in the apical membranes of polarized cells and is mainly expressed in the liver, intestine and kidney. Comparison of both transporters shows that human MRP1 and MRP2 are composed of 1531 and 1545 amino acids, respectively. They exhibit an amino acid identity of 49% with the highest degree of amino acid identity in the carboxyl-terminal domain and in both nucleotide-binding domains [2,12]. Despite this limited amino acid identity, the spectrum of substrates transported by MRP1 and MRP2 overlap to a large extent although MRP1 seems to be less specific [13–15]. It has been shown that over-expression of not only MRP1, but also MRP2, confers multidrug resistance characterized by resistance to a broad spectrum of anticancer agents (reviewed in [16]). Identification of MRP1 and MRP2 mediated transport as important mechanisms in multidrug resistance during cancer treatment led to the search for agents that could reverse resistance due to the activity of these transporters. One of the possible strategies for reversal of MRP mediated multidrug resistance is inhibition of the activity of these proteins. Several inhibitors of MRP1 and MRP2 have been described in the literature. These inhibitors are mostly relatively non-specific inhibitors of organic anion transport, like sulfinpyrazone, benzbromarone and probenecid [3,11]. Many MRP1 inhibitors, like certain tricyclic isoxazoles, do inhibit MRP1 in intact cells at micromolar concentrations but they are much less active against MRP2 [17,18]. Another important feature is that some inhibitors, like the leukotriene D<sub>4</sub> receptor antagonist MK571, is an excellent MRP1 inhibitor in vesicular transport experiments, but is less efficient regarding MRP1 inhibition in intact cells [17].

The quest for transport inhibitors showed that many natural constituents, including plant polyphenols like flavonoids were promising candidates for possible MRP1 inhibition [19–24]. Flavonoids are a large group of polyphenolic antioxidants found in fruits and vegetables. Although the literature points at possible inhibition of MRP1 activity by flavonoids, the relation between the chemical structure and the MRP1 inhibitory potency has hardly been described. For MRP2, up to date no studies regarding the effects of flavonoids on its activity have been described.

In the present study, the effects of a large series of flavonoids (Fig. 1) on either the MRP1, or MRP2 mediated efflux of calcein in transfected MDCKII cells were examined. The results were used to derive quantitative structure activity relationships (QSAR) to quantitatively describe the structural requirements of flavonoids necessary for potent MRP1 and MRP2 inhibition in a cellular model system. These results provide insight in the structural characteristics involved in MRP inhibition and explore the differences between inhibitors of these two transporters, MRP1 and MRP2.

## 2. Materials and methods

### 2.1. Materials

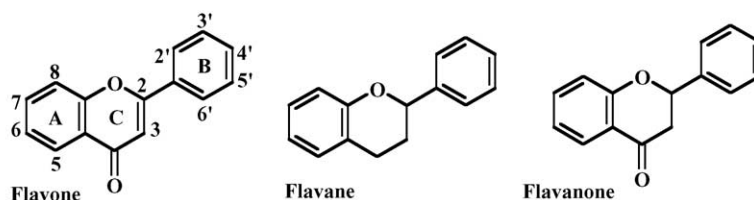
The Madin-Darby canine kidney (MDCKII) cell lines, stably expressing either a control vector (hereafter called control cells), human *MRP1* cDNA (hereafter called MRP1 cells) [25] or *MRP2* cDNA (hereafter called MRP2 cells) [15] were kindly provided by Prof. P. Borst (NKI, Amsterdam).

Dulbecco's minimum essential medium (DMEM) with GlutaMax, fetal calf serum, penicillin/streptomycin and gentamycin were all from Gibco. MK571 was obtained from BioMol; PSC833 was a kind gift from Novartis Pharma AG. Cyclosporin A was from Fluka. Calcein acetoxymethyl ester (calcein-AM) was obtained from Molecular Probes. Morin, 3-hydroxyflavone, galangin, flavone and apigenin were purchased from Aldrich. Taxifolin, chrysin, naringenin, acacetin, 3'-hydroxyflavone, 4'-hydroxyflavone, 3,3'-dihydroxyflavone, 3,3',4'-trihydroxyflavone, robinetin, isorhamnetin and catechin were obtained from Indofine. Luteolin, myricetin and quercetin were purchased from Sigma Chemical Co. HPLC grade methanol was obtained from Labscan and HPLC grade trifluoro acetic acid (TFA) was obtained from Baker. Eriodictyol, kaempferol, baicalein, kaempferide, 5,7,3',4'-tetramethoxyluteolin, diosmetin, chrysoeriol, tamarixetin were purchased from Extrasynthese.

#### 2.1.1. MDCKII cell culture

The Madin-Darby canine kidney cell lines (control and MRP1 or MRP2 transfected) were cultured in Dulbecco's minimum essential medium (DMEM) with GlutaMax (4.5 g glucose per liter), 10% fetal calf serum and 0.01% penicillin/streptomycin, and were grown in a humidified atmosphere of 5% CO<sub>2</sub> at 37 °C.

For transport experiments  $4 \times 10^5$  cells/cm<sup>2</sup> were grown on microporous polycarbonate filters (0.4 μm pore size, 4.7 cm<sup>2</sup>; Costar Corp.). It was shown earlier that in these polarized cell lines MRP1 routes to the basolateral plasma membrane, whereas MRP2 routes to the apical plasma membrane. Culturing MDCKII cells on a filter in transwells provides the opportunity to study both the MRP1- or MRP2-mediated efflux of the parent compound and/or its metabolites to either the apical or basolateral side of intact cells. The volume of media in the basolateral and apical compartments was 1.8 and 0.5 ml, respectively. Cells were cultured to confluency for three days and medium was replaced every 24 h. Confluency of the monolayers was checked by transepithelial electric resistance (TEER) measurement. TEER-values of each monolayer were measured using a Millicell-ERS epithelial volt/ohm meter (Millipore). The TEER-value of a confluent monolayer of MDCKII cells ranged between 200–250 Ω cm<sup>2</sup> as reported before [26]. The leukotriene D<sub>4</sub> receptor antagonist MK-571 was used as a typical MRP1 inhibitor [27] and



Flavonoid	Class	Hydroxylation Pattern	Methoxylation Pattern
Flavone	Flavone	-	
3-Hydroxyflavone	Flavone	3	
3'-Hydroxyflavone	Flavone	3'	
4'-Hydroxyflavone	Flavone	4'	
Chrysin	Flavone	5,7	
3,3'-Dihydroxyflavone	Flavone	3, 3'	
3',4'-Dihydroxyflavone	Flavone	3', 4'	
Galangin	Flavone	3,5,7	
Baicalein	Flavone	5,6,7	
Apigenin	Flavone	5,7,4'	
Naringenin	Flavanone	5,7,4'	
3,3',4'-Trihydroxyflavone	Flavone	3,3',4'	
Kaempferol	Flavone	3,5,7,4'	
Fisetin	Flavone	3,7,3',4'	
Luteolin	Flavone	5,7,3',4'	
Eriodictyol	Flavanone	5,7,3',4'	
Morin	Flavone	3,5,7,2',4'	
Quercetin	Flavone	3,5,7,3',4'	
Taxifolin	Flavanone	3,5,7,3',4'	
Catechin	Flavane	3,5,7,3',4'	
Robinetin	Flavone	3,7,3',4',5'	
Myricetin	Flavone	3,5,7,3',4',5'	
Acacetin	Flavone	5,7	4'
Kaempferide	Flavone	3,5,7	4'
5,7,3',4'-Tetramethoxyflavone	Flavone		5,7,3',4'
Diosmetin	Flavone	5,7,3'	4'
Chrysoeriol	Flavone	5,7,4'	3'
Tamarixetin	Flavone	3,5,7,3'	4'
Isorhamnetin	Flavone	3,5,7,4'	3'

Fig. 1. The model flavonoids used in the present study.

cyclosporin A was used as a typical MRP2 inhibitor [13].

### 2.1.2. Efflux of calcein in MDCKII cells

The efflux of calcein, which is a good substrate for MRP1 and MRP2, was determined using confluent monolayers of control, MRP1 and MRP2 cells. First cells cultured on 12 mm diameter transwells (Costar Corp.) were loaded with the calcein-AM at a final concentration of 1  $\mu\text{M}$  in DMEM without phenol red for 2 h at 7  $^{\circ}\text{C}$ . Calcein-AM uptake and intracellular conversion to calcein in these MDCKII cell lines has been described before [28]. For the kinetic characterization of calcein efflux inhibition by flavonoids, several calcein-AM concentrations were used: 1, 0.5, 0.1 and 0.05  $\mu\text{M}$ . At these calcein-AM concentrations the efflux of calcein by MRPs is not saturated since the calcein efflux was a linear function of the calcein-AM concentration. The calcein-AM concentration used for the QSAR studies (1  $\mu\text{M}$ ) was based upon previous studies by our group where 1  $\mu\text{M}$  calcein-AM

appeared to be a very suitable concentration for inhibition studies [28]. Essodaigui et al. described that calcein-AM equilibrates very rapidly over the cellular plasma membrane, resulting in similar inside and outside concentrations of calcein-AM [29]. Once inside the cells, cleavage of this non-fluorescent calcein-AM ester by intracellular esterases leads to formation of the fluorescent derivative calcein. The non-fluorescent calcein-AM, is a good substrate for both P-glycoprotein (P-gp) and MRP1 [30]. To diminish the MRP-dependent efflux of calcein-AM—and because it was preferred to use no MRP inhibitors during loading time—cells were loaded with calcein-AM at a temperature of 7  $^{\circ}\text{C}$ . In addition, PSC833 (0.1  $\mu\text{M}$ ) was added as P-gp inhibitor. After the 3-h loading, the cells were washed three times with DMEM without phenol red (37  $^{\circ}\text{C}$ ) during approximately 10 min. The efflux experiments were started by exposing the cells to fresh medium (37  $^{\circ}\text{C}$ ) containing 0.1  $\mu\text{M}$  PSC833 and different concentrations of flavonoids (1, 10, 20, 30, 40 and 50  $\mu\text{M}$ ) or 50  $\mu\text{M}$  MK571 (as a typical MRP1 inhibitor), or 30  $\mu\text{M}$

cyclosporin A (as a typical MRP2 inhibitor) in both, apical and basolateral, compartments. Fig. 1 lists the various flavonoids tested. Cells receiving vehicle only (0.5% DMSO, v/v) served as control. The highest flavonoid concentrations tested were 50  $\mu\text{M}$ , because some flavonoids are either cytotoxic or poorly soluble at concentrations above 50  $\mu\text{M}$ . Efflux of calcein was measured in media samples from both the apical and basolateral compartment at  $t = 0, 25$  and 45 min and the level of calcein in the intracellular compartment before and after the efflux experiments. Fluorescence of the samples was determined using a Varian Cary Eclipse (Varian) with excitation at 485 nm and emission at 530 nm. The fluorescence of the samples was corrected for the minor changes in background fluorescence caused by the flavonoids. Analysis of the calcein concentrations in the apical, basolateral and intracellular compartments at  $t = 0$  and 45 min of the efflux experiments showed that during the efflux experiments no significant increase in total calcein amounts was observed (data not shown). Apparently, all calcein-AM taken up in the cells during loading is converted into calcein during the loading period and/or the period for washing of the cells before the efflux experiments start.

$\text{IC}_{50}$  values were obtained via curve fitting using the Microsoft Excel data analysis V1.1 toolpack.

#### 2.1.3. High Performance Liquid Chromatography (HPLC) analysis of flavonoid lipophilicity

To determine the relative lipophilicity of the flavonoids, HPLC was carried out using a Thermo Finnigan HPLC system equipped with a P200 pump and an AS 3000 autosampler. Flavonoids were freshly prepared at a final concentration of 100  $\mu\text{M}$  in DMEM without phenol red, and 50  $\mu\text{l}$  of this solution were injected onto a 150 mm  $\times$  4.6 mm Alltech Alltima C18 column. The isocratic mobile phase consisted of 0.1% trifluoroacetic acid and methanol (4.5:5.5 v/v) and elution was carried out at a flow rate of 1 ml/min. Detection was performed by measuring the absorbance at 254 nm using a Thermo Finnigan UV 100 detector. The lipophilicity of the flavonoids was calculated using the capacity factor ( $K'$ ), calculated by:  $K' = (t_r - t_0)/t_0$ , in which:  $K'$  = capacity factor,  $t_r$  = retention time of the flavonoid (min) and  $t_0$  = retention time of unretained substances (min).

#### 2.1.4. Molecular characteristics of flavonoid structures

To quantify the relative effects of the C2–C3 double bond, hydroxyl and methoxylated moieties on the planarity of the flavonoid molecules the dihedral angle between the B- and C-ring was calculated using computational modeling carried out on a Silicon Graphics Indigo workstation using Spartan 5.0 (Wavefunction Inc.). Each molecule was built in Spartan and its geometry was optimized by the semi-empirical PM3 method. After optimization, the C3–C2–C1'–C2' dihedral angles were measured. Other descriptors evaluated besides the dihedral angle were:

lipophilicity (determined experimentally as  $K'$ ), total number of hydroxyl groups, the number of hydroxyl groups on the A-, B- or C-ring of the flavonoid, the presence of catechol moieties (two adjacent hydroxyl groups) or pyrogallol moieties (three adjacent hydroxyl groups) and the number of methoxylated groups on the flavonoid.

#### 2.1.5. Data analysis

Descriptive and inferential statistical analyses were performed. The hypothesis of normality was evaluated by the Shapiro-Wilks test. Correlation analysis was evaluated by Spearman's non-parametric correlation analysis. Stepwise multiple regression analysis was used to describe the relation between the percentage MRP inhibition and the main important descriptors in a regression model (QSAR). Models obtained were statistically tested by variance analysis using ANOVA ( $P < 0.05$ ). Least square regression analysis was used to determine the correlation between the measured data and the expected (calculated) data from the model (adapted from [31]). All analyses have been performed using SPSS 10.1.0 software from SPSS Inc.

### 3. Results

#### 3.1. MRP1 and MRP2 efflux characteristics and inhibition

The inhibition of MRP1 and MRP2 activity was studied using the fluorescent calcein as a model substrate. After

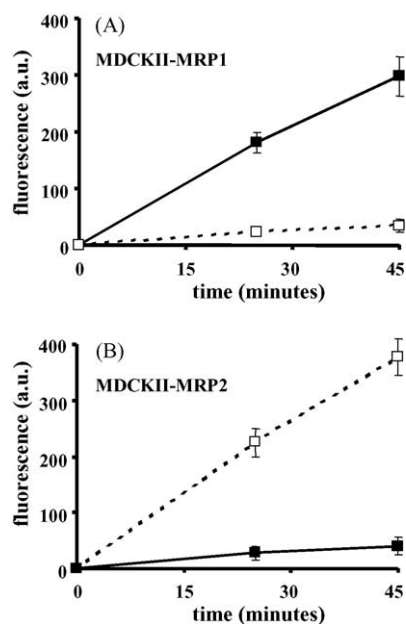


Fig. 2. Typical time-dependent efflux patterns of calcein by MDCKII-MRP1 (A) and MDCKII-MRP2 cells (B). Open symbols ( $\square$ ) represent efflux to the apical compartment, closed symbols ( $\blacksquare$ ) represent efflux to the basolateral compartment. Each point represents the average  $\pm$  S.D. from triplicate measurements.

Table 1

The percentage inhibition after exposure to 25  $\mu\text{M}$  of the tested flavonoids and determined  $\text{IC}_{50}$  values for both MRP1 and MRP2

	MRP1		MRP2	
	Inhibition at 25 $\mu\text{M}$ (%)	$\text{IC}_{50}$ ( $\mu\text{M}$ )	Inhibition at 25 $\mu\text{M}$ (%)	$\text{IC}_{50}$ ( $\mu\text{M}$ )
Flavone	36	>50	5	>50
3-Hydroxyflavone	3	>50	2	>50
3'-Hydroxyflavone	13	>50	0	>50
4'-Hydroxyflavone	15	>50	1	>50
Chrysin	10	>50	2	>50
3,3'-Dihydroxyflavone	4	>50	1	>50
3',4'-Dihydroxyflavone	57	24.4 $\pm$ 4.1	16	>50
Galangin	43	35.3 $\pm$ 7.3	0	>50
Baicalein	48	30.9 $\pm$ 4.4	28	>50
Apigenin	47	35.1 $\pm$ 9.6	2	>50
Naringenin	2	>50	0	>50
3,3',4'-Trihydroxyflavone	26	>50	17	>50
Kaempferol	72	19.4 $\pm$ 3.6	2	>50
Fisetin	2	>50	1	>50
Luteolin	53	22.4 $\pm$ 4.8	17	>50
Eriodictyol	31	>50	13	>50
Morin	30	49.0 $\pm$ 7.6	8	>50
Quercetin	63	21.8 $\pm$ 3.5	5	>50
Taxifolin	8	>50	3	>50
Catechin	15	>50	0	>50
Robinetin	75	13.6 $\pm$ 3.9	76	15.0 $\pm$ 3.5
Myricetin	63	20.2 $\pm$ 4.3	68	22.2 $\pm$ 3.9
Acacetin	18	>50	1	>50
Kaempferide	40	>50	2	>50
5,7,3',4'-Tetramethoxyflavone	76	7.9 $\pm$ 1.5	20	>50
Diosmetin	84	2.7 $\pm$ 0.6	17	>50
Chrysoeriol	85	4.0 $\pm$ 0.7	31	>50
Tamarixetin	68	7.4 $\pm$ 3.4	8	>50
Isorhamnetin	60	14.3 $\pm$ 2.8	10	>50

When no  $\text{IC}_{50}$  values could be obtained using concentrations up to 50  $\mu\text{M}$  this is indicated by >50. Values were obtained by curve fitting analysis using data measured in triplo.

loading the cells with the non-fluorescent calcein-AM that is converted to the fluorescent MRP-substrate calcein by intracellular esterases, the efflux of calcein was measured in the absence or presence of flavonoids. Fig. 2 shows the typical time-dependent efflux patterns of calcein by MDCKII-MRP1 and MDCKII-MRP2 cells. In MRP1 cells, calcein is predominantly excreted to the basolateral side (eight times higher than apical efflux), whereas in MRP2 cells the efflux of calcein is predominantly to the apical side (11 times higher than basolateral efflux). The presence of the P-gp inhibitor PSC833 did not affect the efflux of calcein by MRP1 and MRP2 (data not shown).

The percentage inhibition upon exposure to 25  $\mu\text{M}$  flavonoid was determined in both cell lines ( $t = 45$  min), and is presented in Table 1. This reveals that most flavonoids are able to inhibit MRP1 activity with varying relative inhibitory potencies. Strikingly, the methoxylated flavonoids 5,7,3',4'-tetramethoxyflavone, diosmetin, chrysoeriol, tamarixetin and isorhamnetin are among the best MRP1 inhibitors, except for kaempferide and acacetin which are less potent inhibitors than the other methoxylated flavonoids. Other flavonoids able to inhibit more than 50% of the MRP1 activity at 25  $\mu\text{M}$  concentrations, were 3',4'-dihydroxyflavone, luteolin, quercetin, robinetin and myricetin. Some of the flavonoids tested inhibited MRP1

activity less than 20%. This group consists of 3-hydroxyflavone, 3'-hydroxyflavone, 4'-hydroxyflavone, chrysin, 3,3'-dihydroxyflavone, naringenin, fisetin, taxifolin and catechin.

In contrast to the wide variety of MRP1 inhibiting flavonoids, only a few of the tested flavonoids inhibited MRP2 mediated calcein efflux at 25  $\mu\text{M}$  concentrations. Most profound effects were found for robinetin and myricetin, which inhibited MRP2 activity more than 50% at 25  $\mu\text{M}$  concentrations.

Fig. 3 shows inhibition curves for the MRP1 mediated basolateral calcein efflux by two flavonoids: robinetin and taxifolin. Robinetin shows a typical concentration dependent inhibition of calcein efflux, whereas taxifolin does not inhibit MRP1 activity. From these and similar curves obtained for all other flavonoids,  $\text{IC}_{50}$  values for the MRP1 and MRP2 activity were determined using flavonoid concentrations up to 50  $\mu\text{M}$  (Table 1). In some cases for MRP1, and almost all for MRP2, it was not possible to derive an  $\text{IC}_{50}$  due to limited inhibition. Again, the methoxylated flavonoids are among the best MRP1 inhibitors with  $\text{IC}_{50}$  values between 2.7 (diosmetin) and 14.3  $\mu\text{M}$  (isorhamnetin). Other potent MRP1 inhibitors were robinetin and myricetin ( $\text{IC}_{50}$  values of 13.6 and 20.2  $\mu\text{M}$ ), kaempferol ( $\text{IC}_{50}$  of 19.4  $\mu\text{M}$ ) as well as quercetin, luteolin

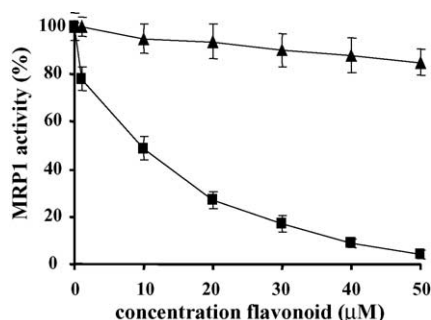


Fig. 3. Inhibition of calcein efflux by MDCKII-MRP1 cells after 45 min exposure to robinetin (■) and taxifolin (▲) as examples of the effects of flavonoids on MRP1 activity. Cells were loaded with calcein-AM at a final concentration of 1  $\mu\text{M}$  for 2 h at 7  $^{\circ}\text{C}$  after which calcein efflux was measured at 37  $^{\circ}\text{C}$ . The results are the mean  $\pm$  S.D. from triplicate measurements.

and 3',4'-dihydroxyflavone ( $\text{IC}_{50}$  of 21.8, 22.4, 24.4  $\mu\text{M}$ , respectively). Especially the flavonoids with only a few or no hydroxyl groups, and the flavonoids lacking a C2–C3 double bond are the least potent MRP1 inhibitors. For MRP2, only robinetin and myricetin were able to inhibit the activity by more than 50% with  $\text{IC}_{50}$  values of 15.0 and 22.2  $\mu\text{M}$ . All other flavonoids did not reach 50% MRP2 inhibition using concentrations up to 50  $\mu\text{M}$ . Clearly, the presence of the flavonol B-ring pyrogallol group results in potent MRP2 inhibition as seen for robinetin and myricetin. Also the presence of an A-ring pyrogallol group, as seen in baicalein, results in minor inhibition (28% at 25  $\mu\text{M}$ ).

### 3.2. MRP1 and MRP2 efflux kinetics

To gain more insight in the mechanism of inhibition, the kinetic parameters (apparent  $K_m$  and apparent  $K_i$ ) for inhibition of calcein efflux by robinetin were determined using Lineweaver-Burk plots based on calcein-AM concentrations used during loading of the cells. Robinetin was taken as a model inhibitor because it appeared to be the flavonoid that most effectively inhibits both MRP1 and MRP2. Fig. 4 shows the Lineweaver-Burk plots for calcein efflux at six different robinetin concentrations in MDCKII-MRP1 (A) and MDCKII-MRP2 (B) cells. These plots reveal a typical competitive inhibition pattern. Using these plots the apparent  $K_m$  calcein and apparent  $K_i$  robinetin for both transporter proteins were calculated. For MRP1, the apparent  $K_m$  calcein was  $0.13 \pm 0.1 \mu\text{M}$ . The apparent  $K_m$  calcein of MRP2 was  $0.40 \pm 0.2 \mu\text{M}$ . The calculated inhibition constants for robinetin, apparent  $K_i$ , were  $5.0 \pm 1.0 \mu\text{M}$  for MRP1 and  $8.5 \pm 1.3 \mu\text{M}$  for MRP2.

### 3.3. Molecular characteristics of flavonoid structures

To elucidate the structural characteristics of flavonoids necessary for potent inhibition of MRP1 and MRP2 various physical and chemical parameters were quantified. The

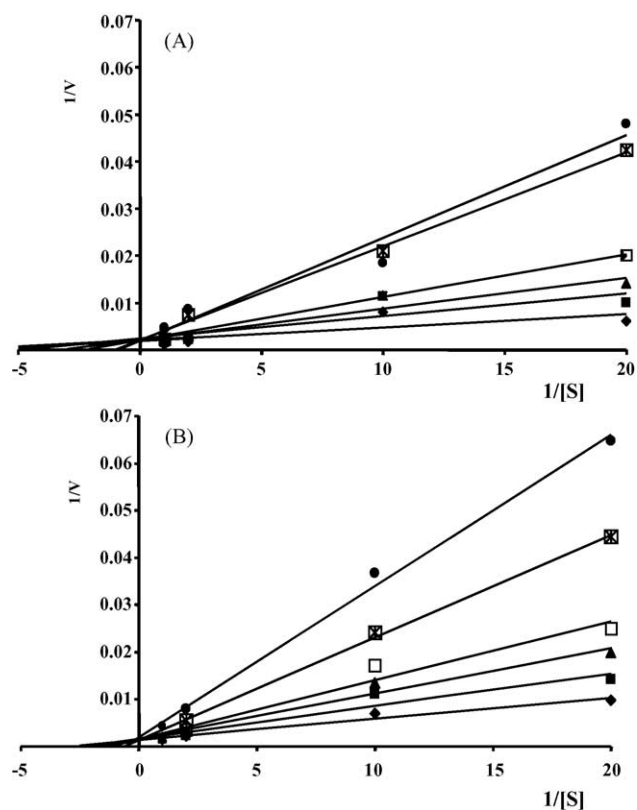


Fig. 4. Lineweaver-Burk plots for MRP-mediated transport activity in the presence of six different robinetin concentrations in MDCKII-MRP1 (A) and MDCKII-MRP2 (B) cells. The reciprocal assumed calcein concentration ( $\mu\text{M}$ ) is plotted on the x-axis, the reciprocal velocity (in A.U. of fluorescence/min/monolayer in the medium) is plotted on the y-axis. The results are the means from duplicate measurements.

characteristics of interest were: lipophilicity, dihedral angle between the B- and C-ring, total number of hydroxyl groups, the number of hydroxyl groups on the A-, B- or C-ring of the flavonoid, the presence of catechol moieties (two adjacent hydroxyl groups) or pyrogallol moieties (three adjacent hydroxyl groups) and the number of methoxylated groups on the flavonoid. Fig. 1 summarizes several of these parameters for the different flavonoids. Table 2 lists two other parameters for all flavonoids tested: the dihedral angle between the B- and C-ring and the lipophilicity reflected by  $K'$ , derived from HPLC elution profiles. The dihedral angle between the B- and C-ring of a flavonoid quantifies the planarity of the flavonoid molecules. These data confirm that saturation of the C2–C3 double bond results in a major change in the dihedral angle, as seen for eriodictyol, taxifolin, catechin and naringenin.

### 3.4. Flavonoid characteristics for potent MRP1 inhibition

To identify and quantify the effects of the different molecular descriptors (structural characteristics) for potent MRP1 inhibition, stepwise multiple regression was performed. The data of Fig. 1 and Tables 1 and 2 were used to derive multiple parameter QSAR models. First, a one-parameter model for each descriptor was derived. Table 3

Table 2  
The measured lipophilicity ( $K'$ ) and calculated dihedral angle between the B- and C-ring for all flavonoids tested

	Lipophilicity ( $K'$ )	Dihedral angle (degrees)
Flavone	19.7	5.5
3-Hydroxyflavone	21.3	14.0
3'-Hydroxyflavone	33.9	7.8
4'-Hydroxyflavone	8.5	3.8
Chrysin	20.9	4.2
3,3'-Dihydroxyflavone	9.5	13.1
3',4'-Dihydroxyflavone	5.5	4.7
Galangin	18.3	14.5
Baicalein	9.1	5.4
Apigenin	11.0	5.7
Naringenin	3.8	39.9
3,3',4'-Trihydroxyflavone	4.5	21.0
Kaempferol	8.8	14.4
Fisetin	2.4	14.4
Luteolin	6.1	7.3
Eriodictyol	2.1	41.9
Morin	2.8	19.3
Quercetin	4.4	14.7
Taxifolin	0.7	36.1
Catechin	2.9	38.8
Robinetin	1.0	15.4
Myricetin	2.1	14.2
Acacetin	28.0	6.7
Kaempferide	32.4	14.0
5,7,3',4'-Teramethoxyflavone	20.4	9.1
Diosmetin	12.1	7.1
Chrysoeriol	11.1	2.3
Tamarixetin	7.2	11.9
Isorhamnetin	10.4	13.9

lists the partial correlation coefficients and  $P$ -values for each one-parameter model. In this model, MRP1 inhibition was best predicted by the number of methoxylated moieties ( $R = 0.427$ ,  $P = 0.021$ ). Thereafter, two-parameter models were derived based on the best one-parameter model. For the two-parameter model, the second best descriptor appeared to be the total number of hydroxyl groups ( $R = 0.586$ ,  $P = 0.040$ ) (Table 3). Consecutively, three-parameter models were derived based on the best two-parameter model (Table 3). The optimal three-parameter model ( $R = 0.766$ ,  $P < 0.001$ ) describing MRP1 inhibition by flavonoids uses the following descriptors: the number of methoxylated moieties, the number of hydroxyl groups and

Table 3

Partial correlation coefficients and  $P$ -values for the three consecutive multi-parameter models: one-parameter model, two-parameter model and three-parameter model describing MRP1 inhibition by flavonoids

	One-parameter model		Two-parameter model		Three-parameter model	
	Partial correlation coefficient	$P$	Partial correlation coefficient	$P$	Partial correlation coefficient	$P$
No. of OCH <sub>3</sub> groups	0.427	0.021	1st Parameter	–	1st Parameter	–
No. of OH groups	0.010	0.960	0.586	0.040	2nd Parameter	–
Log dihedral angle	0.296	0.118	0.484	0.234	0.766	<0.001
Log $K'$	0.233	0.223	0.210	0.047	0.607	0.080
No. of pyrogallol and catechol moieties	0.031	0.872	0.466	0.041	0.586	0.013

The optimal three-parameter model obtained was: % inhibition = 45.466 + 18.936 (no. of OCH<sub>3</sub> moieties) + 12.474 (no. of OH groups) – 48.246 (log dihedral angle).

the dihedral angle between the B- and C-ring and is described by Eq. (1);

$$\begin{aligned} \% \text{ inhibition} = & 45.466 + 18.936 (\text{no. of OCH}_3 \text{ moieties}) \\ & + 12.474 (\text{no. of OH groups}) \\ & - 48.246 (\text{log dihedral angle}). \end{aligned} \quad (1)$$

Other descriptors like lipophilicity and the presence of catechol and pyrogallol moieties did not significantly improve the model. Fig. 5 displays the relation between the measured inhibition of MRP1 activity and the inhibition calculated by Eq. (1) for all flavonoids tested. Least square regression analysis reveals a correlation coefficient of 0.766.

### 3.5. Flavonoid characteristics for potent MRP2 inhibition

Due to the limited number of flavonoids that were able to inhibit MRP2 activity and the limited inhibition caused by the flavonoids tested, the identification of structural characteristics necessary for potent MRP2 inhibition is straightforward but not complete. The presence of a flavonol B-ring pyrogallol group results in potent MRP2 inhibition as seen for robinetin and myricetin. The presence of an A-ring pyrogallol group, as seen in baicalein, results in minor inhibition (28% at 25  $\mu\text{M}$ ). As a consequence, multiple regression analysis resulted in only one significant model: a single-component model ( $R = 0.408$ ,  $P = 0.028$ ) with the total number of pyrogallol and/or catechol moieties as descriptor (Table 4).

## 4. Discussion

The results reported in the present study describe structural characteristics of flavonoids responsible for high potency MRP1 or MRP2 inhibition. MRP1 and MRP2 are well known members of the MRP family, all ATP-binding cassette transporters. Despite the limited amino acid identity, the spectrum of substrates transported by MRP1 and MRP2 overlap to a large extent. The two transporters may differ in affinity towards their substrates. As an example, MRP1 exhibits, in comparison to MRP2, a 10-fold higher  $K_m$  to leukotriene

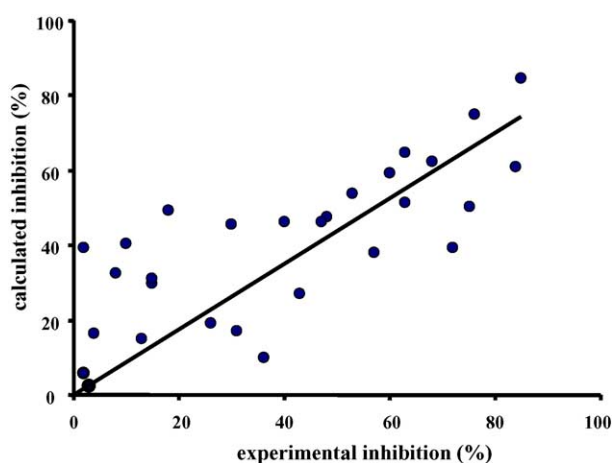


Fig. 5. The relation between the measured inhibition and predicted (calculated) inhibition of MRP1 activity for all flavonoids tested ( $R = 0.766$ ,  $P < 0.001$ ) using the equation: % inhibition =  $45.466 + 18.936$  (no. of  $\text{OCH}_3$  moieties) +  $12.474$  (no. of OH groups) –  $48.246$  (log dihedral angle).

C4 (LTC4) and a five-fold higher  $K_m$  to  $17\beta$ -estradiol-( $\text{D}$ -glucuronide) [14]. The apparent  $K_m$  of both proteins towards the substrate used in this study, calcein, differs marginally, being  $0.13 \pm 0.1 \mu\text{M}$  for MRP1 and  $0.40 \pm 0.2 \mu\text{M}$  for MRP2, based on calcein-AM concentrations used during loading of the cells.

The outcomes of this study show that MRP1 is far more susceptible to inhibition by flavonoids than MRP2 (summarized in Table 1). The methoxylated flavonoids 5,7,3',4'-tetramethoxyflavone, diosmetin, chrysoeriol, tamarixetin and isorhamnetin are among the best MRP1 inhibitors as indicated by their low  $\text{IC}_{50}$  values, ranging between 2.7 and  $14.3 \mu\text{M}$ . Interestingly, these  $\text{IC}_{50}$  values are in the same range or slightly above the  $\text{IC}_{50}$  value of  $5 \mu\text{M}$  of the typical MRP1 inhibitor MK571, measured in the same cellular system [28]. Other flavonoids able to inhibit more than 50% of MRP1 activity were 3',4'-dihydroxyflavone, luteolin, quercetin, robinetin and myricetin with  $\text{IC}_{50}$  values ranging between 13.6 and  $24.4 \mu\text{M}$ . In contrast to the wide variety of flavonoids able to inhibit MRP1, only a few of the tested flavonoids were able to inhibit MRP2 mediated efflux. Only robinetin and myricetin were able to inhibit MRP2 activity more than 50%, with  $\text{IC}_{50}$  values of 15.0 and  $22.2 \mu\text{M}$ , respectively. Again, these  $\text{IC}_{50}$

values are in the same range as reported for the typical MRP2 inhibitor, cyclosporine A, for which the  $\text{IC}_{50}$ , measured under identical experimental conditions, was  $10 \mu\text{M}$  [28]. Apparently, robinetin and myricetin possess comparable MRP2-inhibitory potencies as the typical MRP2 inhibitor cyclosporin A.

The competitive nature of calcein efflux inhibition by robinetin indicates that robinetin binds to the same binding site on MRP1 and MRP2 as calcein. Competitive inhibition of MRP1 by flavonoids has been reported before for LTC4 transport in reconstituted vesicles [21]. The kinetic studies of MRP1 and MRP2 efflux inhibition by robinetin resulted in calculated apparent inhibition constants  $K_i$  robinetin. These apparent constants were almost similar:  $5.0 \mu\text{M}$  for MRP1 and  $8.5 \mu\text{M}$  for MRP2. Determination of apparent  $K_i$  values for flavonoid mediated MRP1 or MRP2 inhibition in a cellular system has not been described before. In a cellular system, the apparent  $K_i$  values might be influenced by cellular processes including, among others, uptake and metabolism. Nevertheless,  $K_i$  values reported by Leslie et al. [21] on the competitive flavonoid mediated inhibition of MRP1 activity in reconstituted membrane vesicles, using LTC4 as substrate, were in the same order of magnitude ( $2.4\text{--}21 \mu\text{M}$ ).

Multiple regression analysis was used for the identification and quantification of the effects of different structural characteristics regarding potent inhibition of MRP1 and MRP2 activity. For MRP1, an optimal multiple parameter QSAR model was obtained. The resulting QSAR equation (Eq. (1)) reveals that three-structural characteristics are of major importance for MRP1 inhibition: the total number of methoxylated moieties, the total number of hydroxyl groups and the dihedral angle between the B- and C-ring. Using this QSAR equation a correlation ( $R = 0.766$ ) was obtained between the predicted inhibition and the actual measured inhibition ( $P < 0.001$ ). Neither the lipophilicity  $K'$ , nor the total number of catechol and/or pyrogallol moieties significantly influence MRP1 inhibition by flavonoids. Comparison of the flavonoid mediated effects on MRP1 activity from this study with previous studies [21,23,24,32], summarized in Table 5, reveal that both the magnitude and the rank order of MRP1 inhibition by flavonoids varies per study, possibly as a result of the different MRP1 substrates used in the different studies (Table 5). Besides the effect of different substrates, another important difference between the present and the other studies is the use of different in vitro model systems.

Regarding MRP2 mediated calcein efflux inhibition, only the presence of a flavonol B-ring pyrogallol group seems to be an important structural characteristic. Ultimately, MRP2 displays a higher selectivity for flavonoid type inhibition than MRP1.

Several mechanisms in which inhibitors might interact with MRPs have been proposed in the literature. Interaction of flavonoids with MRPs might affect: drug binding, ATP binding, ATP hydrolysis, drug transport, and ADP

Table 4  
Partial correlation coefficients and  $P$ -values for the one-parameter model describing MRP2 inhibition by flavonoids

	Partial correlation coefficient	$P$
No. of $\text{OCH}_3$ groups	0.076	0.697
No. of OH groups	0.364	0.052
Log dihedral angle	0.107	0.579
Log $K'$	0.281	0.148
No. of pyrogallol and catechol moieties	0.408	0.028



Table 5  
Schematic overview of the experimental outline and main results from this study and other related studies

Model system	Pump	Substrate	No. of flavonoids tested	Concentrations ( $\mu\text{M}$ )	$K_i$ ( $\mu\text{M}$ )	Most potent inhibitors	Structural characteristics important for MRP inhibition	Reference <sup>a</sup>
MDCKII cells	MRP1	Calcein	29	0.1–50	5.0 (robinetin)	Diosmetin > chrysoeriol > tamarixetin > tetra-methoxyflavone > robinetin > iso-rhamnetin > kaempferol > myricetin > quercetin > luteolin	Dihedral angle; number of hydroxyl groups; number of methoxylated moieties	This study
MDCKII cells	MRP2	Calcein	29	0.1–50	8.5 (robinetin)	Robinetin > myricetin	Flavonol B-ring pyrogallol moiety	This study
MCF7 cells	GS-X pump	DNP-SG	11	0.1–50	–	Luteolin > quercetin > kaempferol > 3',4'-dihydroxyflavone > myricetin	Hydroxyl groups (especially two of them generating the 3',4'-catechol moiety); dihedral angle	1
Vesicles	MRP1	LTC4	8	1–100	2.4–21 (various)	Kaempferol > apigenin > quercetin > myricetin > naringenin	Not defined	2
Vesicles	MRP1	17 $\beta$ -estradiol	8	1–100	–	Apigenin > kaempferol > naringenin > quercetin > myricetin	Lipophilicity	2
Panc-1 cells	MRP1	Daunomycin/vinblastin	22	100	–	Morin > kaempferol > quercetin > genistein	Not defined	3
Human erythrocytes	Most likely MRP1	BCPCF	30 (mostly modified)	0–100	–	Euchrestafavanone A = sophora-flavanone H > other sophoraflavanones	Flavanones with a prenyl, geranyl or lavandulyl group	4

<sup>a</sup> Used literature: (1) van Zanden et al. [24]; (2) Leslie et al. [21]; (3) Nguyen et al. [23]; (4) Bobrowska-Hagerstrand et al. [32].

release. Flavonoids are well known inhibitors (but sometimes also stimulators) of ATPase activity [21,22,33,34]. Possibly, more than one interaction/effect might take place simultaneously. Another example of such an interaction of flavonoids with MRPs can be found in studies reported for human colonic carcinoma Caco-2 cells [35,36]. These reports show that flavonoids as well as their glucuronide- and sulphate-conjugates and their glycosylated forms can act as MRP2 substrates and are efficiently transported by this transporter. This observation suggests an interaction of flavonoids with the substrate binding site of MRP2. The competitive inhibition of MRP1 and MRP2 mediated transport by robinetin demonstrated in the present study corroborates this conclusion of interaction at the substrate binding site.

In contrast to the possible beneficial use of flavonoids as MDR modulators, the increased intake of extreme doses of flavonoids via dietary supplementation might disturb physiological processes. This increased intake of flavonoids might affect the kinetics of other food constituents, pharmaceuticals, xenobiotics or endogenous substrates of MRPs. Especially in the intestine, high flavonoid concentrations can be expected upon supplementation, since quercetin supplements are known to result in daily intakes up to 1 g/day, plasma levels of up to 10  $\mu\text{M}$  and intestine concentrations that are even higher [37,38]. Comparing these concentrations to the  $\text{IC}_{50}$  values and  $K_i$  values of the present study indicates that the inhibitory effects observed in the present study can be expected to be relevant in vivo as well. Some flavonoids are known to become cytotoxic at concentrations above 50  $\mu\text{M}$  [39,40]. Since the  $\text{IC}_{50}$  values obtained in the present study are 2–20 times lower, the inhibition of MRPs by flavonoids can be obtained at therapeutic non-toxic concentrations. In addition, since the present study used calcein concentrations approximately 2.5–8 times higher than the apparent  $K_m$  of MRPs for calcein efflux, based on calcein-AM concentrations used during loading of the cells, it can be expected that at lower calcein concentrations the corresponding  $\text{IC}_{50}$  values for inhibition by flavonoids will be even lower.

In summary, this study describes the inhibitory interaction of flavonoids with MRP1 and MRP2. Moreover, this study also shows that MRP2 displays a higher selectivity for flavonoid type inhibition than MRP1. Molecular characteristics responsible for these inhibitory actions on MRP1 and MRP2 were identified and, for MRP1, a model was developed quantitatively describing the MRP1 inhibitory potency of flavonoids based on their molecular characteristics.

## Acknowledgements

The authors thank Prof. P. Borst from the National Cancer Institute (Amsterdam, The Netherlands) who kindly provided the transfected MDCKII cell lines and for critically reading the manuscript. This research was financially supported by grant TNOV 2000–2169 of the Dutch Cancer Society.

## References

- [1] Higgins CF. ABC transporters: from microorganisms to man. *Annu Rev Cell Biol* 1992;8:67–113.
- [2] Borst P, Evers R, Koel M, Wijnholds J. A family of drug transporters: the multidrug resistance-associated proteins. *J Natl Cancer Inst* 2000;92(16):1295–302.
- [3] Borst P, Elferink RO. Mammalian abc transporters in health and disease. *Annu Rev Biochem* 2002;71:537–92.
- [4] Borst P, Zelcer N, van Helvoort A. ABC transporters in lipid transport. *Biochim Biophys Acta* 2000;1486(1):128–44.
- [5] Renes J, Vries GE, Jansen LM, Muller M. The (patho)physiological functions of the MRP family. *Drug Resist Updates* 2000;3:289–302.
- [6] Cole SP, Bhardwaj G, Gerlach JH, Mackie JE, Grant CE, Almquist KC, et al. Overexpression of a transporter gene in a multidrug-resistant human lung cancer cell line. *Science* 1992;258(5088):1650–4.
- [7] Loe DW, Deeley RG, Cole SP. Characterization of vincristine transport by the M(r) 190,000 multidrug resistance protein (MRP): evidence for cotransport with reduced glutathione. *Cancer Res* 1998;58(22):5130–6.
- [8] Qian YM, Song WC, Cui H, Cole SP, Deeley RG. Glutathione stimulates sulfated estrogen transport by multidrug resistance protein 1. *J Biol Chem* 2001;276(9):6404–11.
- [9] Renes J, de Vries EG, Nienhuis EF, Jansen PL, Muller M. ATP- and glutathione-dependent transport of chemotherapeutic drugs by the multidrug resistance protein MRP1. *Br J Pharmacol* 1999;126(3):681–8.
- [10] Bagrij T, Klokouzas A, Hladky SB, Barrand MA. Influences of glutathione on anionic substrate efflux in tumour cells expressing the multidrug resistance-associated protein, MRP1. *Biochem Pharmacol* 2001;62(2):199–206.
- [11] Konig J, Nies AT, Cui Y, Leier I, Keppler D. Conjugate export pumps of the multidrug resistance protein (MRP) family: localization, substrate specificity, and MRP2-mediated drug resistance. *Biochim Biophys Acta* 1999;1461(2):377–94.
- [12] Keppler D, Konig J. Hepatic canalicular membrane 5: expression and localization of the conjugate export pump encoded by the MRP2 (cMRP/cMOAT) gene in liver. *FASEB J* 1997;11(7):509–16.
- [13] Chen ZS, Kawabe T, Ono M, Aoki S, Sumizawa T, Furukawa T, et al. Effect of multidrug resistance-reversing agents on transporting activity of human canalicular multispecific organic anion transporter. *Mol Pharmacol* 1999;56(6):1219–28.
- [14] Cui Y, Konig J, Buchholz JK, Spring H, Leier I, Keppler D. Drug resistance and ATP-dependent conjugate transport mediated by the apical multidrug resistance protein, MRP2, permanently expressed in human and canine cells. *Mol Pharmacol* 1999;55(5):929–37.
- [15] Evers R, Koel M, van Deemter L, Janssen H, Calafat J, Oomen LC, et al. Drug export activity of the human canalicular multispecific organic anion transporter in polarized kidney MDCK cells expressing cMOAT (MRP2) cDNA. *J Clin Invest* 1998;101(7):1310–9.
- [16] Sparreboom A, Danesi R, Ando Y, Chan J, Figg WD. Pharmacogenomics of ABC transporters and its role in cancer chemotherapy. *Drug Resist Updat* 2003;6(2):71–84.
- [17] Norman BH. Inhibitors of MRP1-mediated multidrug resistance. *Drugs Future* 1998;23:1001–13.
- [18] Norman BH, Gruber JM, Hollinshead SP, Wilson JW, Starling JJ, Law KL, et al. Tricyclic isoxazoles are novel inhibitors of the multidrug resistance protein (MRP1). *Bioorg Med Chem Lett* 2002;12(6):883–6.
- [19] Hooijberg JH, Broxterman HJ, Heijn M, Fles DL, Lankelma J, Pinedo HM. Modulation by (iso)flavonoids of the ATPase activity of the multidrug resistance protein. *FEBS Lett* 1997;413(2):344–8.
- [20] Conseil G, Baubichon-Cortay H, Dayan G, Jault JM, Barron D, Di Pietro A. Flavonoids: a class of modulators with bifunctional interactions at vicinal ATP- and steroid-binding sites on mouse P-glycoprotein. *Proc Natl Acad Sci U S A* 1998;95(17):9831–6.
- [21] Leslie EM, Mao Q, Oleschuk CJ, Deeley RG, Cole SP. Modulation of multidrug resistance protein 1 (MRP1/ABCC1) transport and atpase activities by interaction with dietary flavonoids. *Mol Pharmacol* 2001;59(5):1171–80.
- [22] Di Pietro A, Conseil G, Perez-Victoria JM, Dayan G, Baubichon-Cortaya H, Trompiera D, et al. Modulation by flavonoids of cell multidrug resistance mediated by P-glycoprotein and related ABC transporters. *Cell Mol Life Sci* 2002;59(2):307–22.
- [23] Nguyen H, Zhang S, Morris ME. Effect of flavonoids on MRP1-mediated transport in Panc-1 cells. *J Pharm Sci* 2003;92(2):250–7.
- [24] van Zanden JJ, Geraets L, Wortelboer HM, Bladeren PJ, Rietjens IMCM, Cnubben NHP. Structural requirements for the flavonoid mediated modulation of glutathione S-transferase P1-1 and GS-X pump activity in MCF7 breast cancer cells. *Biochem Pharmacol* 2004;67(8):1607–17.
- [25] Evers R, Cnubben NH, Wijnholds J, van Deemter L, van Bladeren PJ, Borst P. Transport of glutathione prostaglandin A conjugates by the multidrug resistance protein 1. *FEBS Lett* 1997;419(1):112–6.
- [26] Irvine JD, Takahashi L, Lockhart K, Cheong J, Tolan JW, Selick HE, et al. MDCK (Madin-Darby canine kidney) cells: a tool for membrane permeability screening. *J Pharm Sci* 1999;88(1):28–33.
- [27] Keppler D, Leier I, Jedlitschky G, Konig J. ATP-dependent transport of glutathione S-conjugates by the multidrug resistance protein MRP1 and its apical isoform MRP2. *Chem Biol Interact* 1998;111–112:153–61.
- [28] Wortelboer HM, Usta M, van der Velde AE, Boersma MG, Spenklink B, van Zanden JJ, et al. Interplay between MRP inhibition and metabolism of MRP inhibitors: the case of curcumin. *Chem Res Toxicol* 2003;16(12):1642–51.
- [29] Essadaoui M, Broxterman HJ, Garnier-Suillerot A. Kinetic analysis of calcein and calcein-acetoxymethyl ester efflux mediated by the multidrug resistance protein and P-glycoprotein. *Biochemistry* 1998;37(8):2243–50.
- [30] Hollo Z, Homolya L, Hegedus T, Muller M, Szakacs G, Jakab K, et al. Parallel functional and immunological detection of human multidrug resistance proteins, P-glycoprotein and MRP1. *Anticancer Res* 1998;18(4C):2981–7.
- [31] Sokal RR, Rohlf FJ. *Biometry*. New York: W.H. Freedman and Company; 1995.
- [32] Bobrowska-Hagerstrand M, Wrobel A, Mrowczynska L, Soderstrom T, Shirataki Y, Motohashi N, et al. Flavonoids as inhibitors of MRP1-like efflux activity in human erythrocytes. A structure–activity relationship study. *Oncol Res* 2003;13(11):463–9.
- [33] Murakami S, Muramatsu M, Tomisawa K. Inhibition of gastric H<sup>+</sup>, K<sup>+</sup>-ATPase by flavonoids: a structure–activity study. *J Enzyme Inhib* 1999;14(2):151–66.
- [34] Boumendjel A, Di Pietro A, Dumontet C, Barron D. Recent advances in the discovery of flavonoids and analogs with high-affinity binding to P-glycoprotein responsible for cancer cell multidrug resistance. *Med Res Rev* 2002;22(5):512–29.
- [35] Walle UK, Galijatovic A, Walle T. Transport of the flavonoid chrysin and its conjugated metabolites by the human intestinal cell line Caco-2. *Biochem Pharmacol* 1999;58(3):431–8.
- [36] Walgren RA, Karnaky Jr KJ, Lindenmayer GE, Walle T. Efflux of dietary flavonoid quercetin 4'-beta-glucoside across human intestinal Caco-2 cell monolayers by apical multidrug resistance-associated protein-2. *J Pharmacol Exp Ther* 2000;294(3):830–6.
- [37] Graefe EU, Derendorf H, Veit M. Pharmacokinetics and bioavailability of the flavonol quercetin in humans. *Int J Clin Pharmacol Ther* 1999;37(5):219–33.
- [38] Hollman PC, vd Gaag M, Mengelers MJ, van Trijp JM, de Vries JH, Katan MB. Absorption and disposition kinetics of the dietary antioxidant quercetin in man. *Free Radic Biol Med* 1996;21(5):703–7.
- [39] Sergediene E, Jonsson K, Szymusiak H, Tyrakowska B, Rietjens IM, Cenas N. Prooxidant toxicity of polyphenolic antioxidants to HL-60 cells: description of quantitative structure–activity relationships. *FEBS Lett* 1999;462(3):392–6.
- [40] Kuntz S, Wenzel U, Daniel H. Comparative analysis of the effects of flavonoids on proliferation, cytotoxicity, and apoptosis in human colon cancer cell lines. *Eur J Nutr* 1999;38(3):133–42.